Faculty of Engineering

Department of Biomedical Engineering

SILK FIBROIN NANOPARTICLES FOR MOLECULAR IMAGING

BME 400/402

GRADUATION PROJECT

Supervisor : Assoc. Prof. Dr. Terin ADALI

Student : İlke Kurt (20092749)

Lefkoşa, 2014

ACKNOWLADGEMENT

This study of carried out at the Department of Biomedical Engineering,Near East University during the 2013-2014 academic year.

First of all, I would like to thank to my supervisor Assoc.Prof.Dr. Terin ADALI for helping and believing me all this time.The words not enough to tell my gratitude to you.

Also special thanks go to Dr.Kaya SÜER, Dr.Mustafa Murat UNCU, Dr.Rasime KALKAN and Meryem GÜVENİR for their valuable comments and help.

I would like to special thank to my parents, Mithat and Ürfet KURT, my sister Burcu for supporting me and believed me all this time. They are always proud with me. I hope I will always make the life better for them.

Finally,thanks to all my friends and colleagues (Öztürk Hakan ZENCİR, Sevim ONGUNER, Ruhsan ONBAŞI, Fatih Veysel NURÇİN, Ahmetcan YALÇIN, Harun ÖZTÜRK) for their friendship, support and for taking my mind out of the work from time to time.

TABLE OF CONTENT

LIST OF FIGURES

LIST OF TABLES

LIST OF ABBREVIATIONS

SF	Silk Fibroin
Ser	Serine
Gly	Glycine
Ala	Alanine
PEG	Polyethylene glycol
MRI	Magnetic Resonans Imaging
SPION	Superparamagnetic iron oxide napoparticles
MNP	Magnetic Nanoparticles
PBS	Phospahate Buffer Saline
ABS	Acetic acid Buffer Saline
KCl	Potassium Chloride
HCl	Hydrochloric Acid
Fe	Iron
NaCl	Sodium Chloride
NaOH	Sodium Hydroxide
TPP	Sodium triphosphate pentabasic
Glys	Glyserine
$CaCl_2$	Calcium Chloride
Na_2CO_3	Sodium Carbonate
CH_3OH	Methanol
$N_2HPO_4.2H_2O$	di-Sodium hydrogen phosphate dehydrate
KH_2PO_4	Potassium dihydrogen phospate
C_2H_5OH	Ethanol
CH_3COOH	Acetic Acid
Fe_2O_3	Magnemite- Iron (II) oxide
Fe_3O_4	Magnetite- Iron(III) oxide

1. INTRODUCTION

Silks are fibrous protein polymer that spun by some arthropods such as silkworms, spiders, mites, scorpions and bees during their metamorphosis [1]. Silk is usually produced within specialized glands after biosynthesis by epithelial cells and secreted from these glands where the proteins are stored prior to spinning into fiber [3].

Silk proteins are preferable in biomedical applications due to their high strength (up to 4.8 GPa), light weight (1.3 g/cm^3) toughness and elasticity (up to 35%) [2] and being block copolimer- linked proteins, highly biocompatible, biodegradable and they can be thermally stable up to 250 ^{0} C. They have also less inflammatory risk and good water vapour permeability. Beside these features it is also it is also economically advantageous to use silk fibroin for biomedical applications.

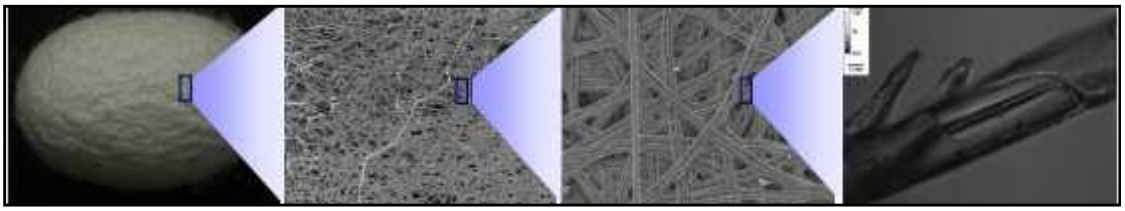

Figure-1.1:Hierarchy of the morphology of a Bombyx mori cocoon.(Scale bar from left to right: 1cm, 200 µm, 20 µm, 10µm)

The most used silks are cocoon silk fibroin from the silkworm Bomboyx mori and silk from a spider Nephila davipes. Silk worm silks are mainly fibroin protein where as the major protein of spider silk is spidroin [4]. The silk based biomaterials are commonly prepared from silk worm silk because it is difficult to get spider silks in the nature.

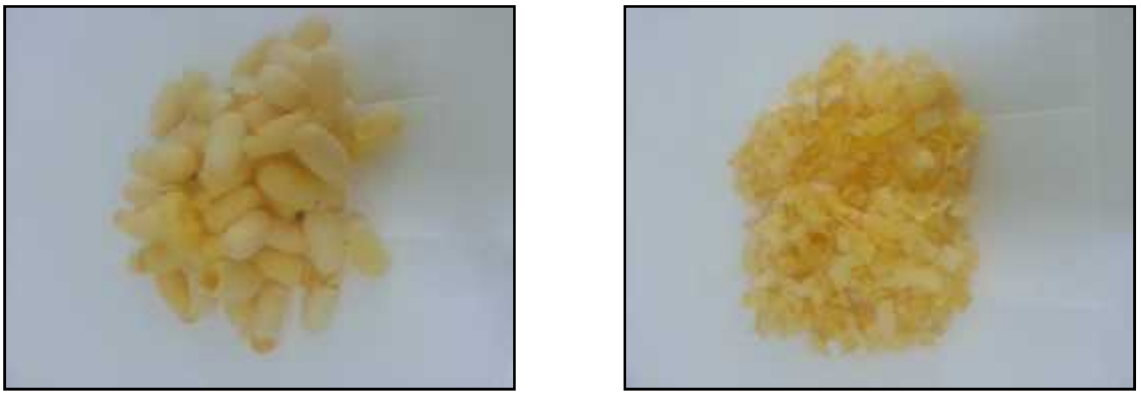

Figure-1.2: The silkworm cocoon

1.1 Silkworm Silk

The silkworm silk is a naturally polymer that has been used in textile production and clinical sutures for centuries [3].

Silkworms live a very short time (about 45-60 days) and liquid silk solution was secreted from large glands in the silkworm. A single silk filament reveals triangular in shape as shown in Figure 3.

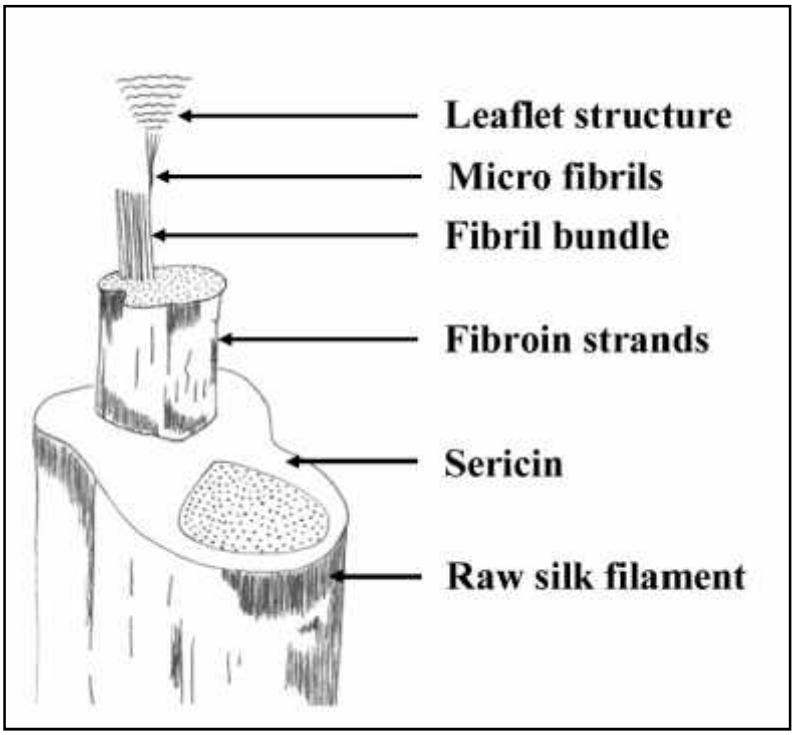

Figure-1.3: Structure of the raw silk fiber [5].

Silk filament is strong has low density and a property of being highly moisture absorbent. Each silk fiber consists of at least two main proteins which are structural protein fibroin and water- soluble glue-like sericin that bind the fibroin fibers together [5].

Silk fibroin (SF) is a natural fibrous protein with semi-crystalline structure which provides stiffness and strength. SF filament consists of heavy (~350 kDa) and light chain (~25 kDa) polypeptides connected by disulfide link [9].

Sericin is an amorphous protein polymer which acts as an adhesive binder to maintain structural integrity of the fibers and the cocoon [1]. It is a complex mixture of 5-6

polypeptides differing in size 40-400 kDa [7]. Silkworm silk must be degummed in order to remove immunogenic sericin coating for biomedical applications.

Silk may contains of bulky amino acids such as glutamic acid, aspartic acid, proline and valine [10]. These amino acids are responsible for the formation of the amorphous part of the silk, which affects the physical properties of the silk with the crystalline region [11].

Amino acid	Fibroin	Sericin
Glycine	42.9	10.5
Alanine	30.0	5.8
Serine	12.2	34
Tyrosine	4.8	3.6
Aspartic acid	1.9	14.6
Arginine	0.5	3.1
Histidine	0.2	1.4
Glutamic acid	1.4	6.2
Lysine	0.4	3.5
Valine	2.5	2.9
Leucine	0.6	0.7
Isoleucine	0.6	0.7
Phenylalanine	0.7	0.4
Proline	0.5	0.6
Threonine	0.9	8.8
Methionine	0.1	0.1
Cystein	Trace	0.1
Tryptophan	-	-

Table-1: Amino acid compositions in silk fiber extracted from mulberry silk (*Bombyx mori*) (g/100 g of fiber) [5].

Silk fiber composes of 75-83% fibroin, 17-25 % sericin, 1.5 % waxes and 1-2 % others such as hydrocarbon by weight [12].

1.2. Silk Fibroin

Silk fibroin is a fibrous protein polymer obtained from the cocoons of domesticated silkworms, such as *Bombyx mori*. Silk fibroin (SF) is amphiphilic because it is characterized as hydrophobic crystalline region and hydrophilic amorphous region [13].

SF filaments consists of heavy chain polypeptides, approximately 325 kDa, and light chain polypeptides, approximately 25 kDa by a single disulfide bond [8]. The heavy chain of SF is comprised of crystalline and amorphous regions. The crystalline region consists of repetitive sequence that form of short side-chain amino acids such as glycine, serine and alanine and the amorphous region consists of larger side-chain bulky amino acids as well as charged amino acids [2].

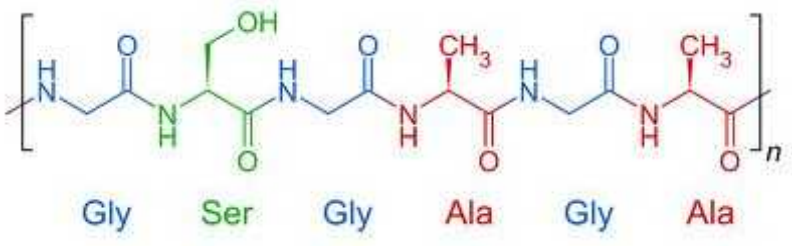

Figure-1.4: Primary structure of fibroin [23].

The hydrophobic blocks tend to form anti-parallel β-sheet secondary structures or crystals through hydrogen bonding and hydrophobic interactions, forming the basis for the tensile strength of silk fibroin. These crystalline regions combine with the amorphous regions to give elasticity and toughness of silk fibroin.

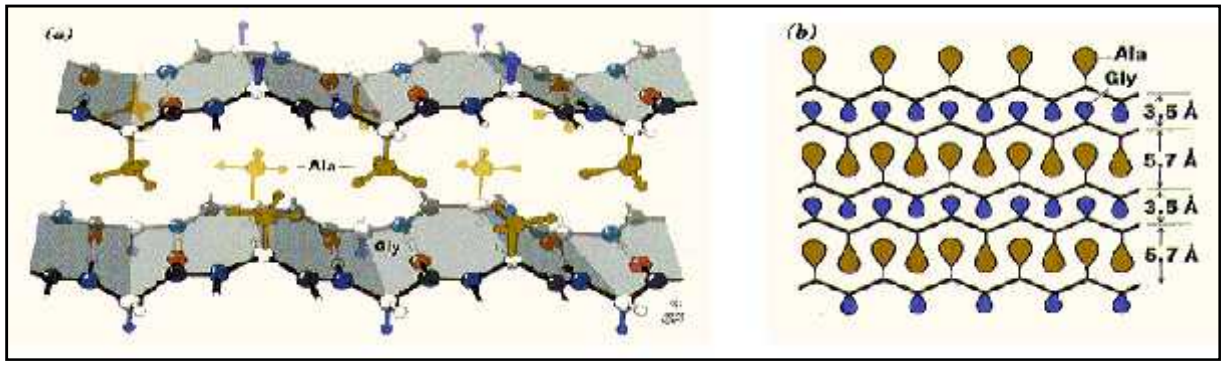

Figure-1.5: β-sheet structure of SF [24].

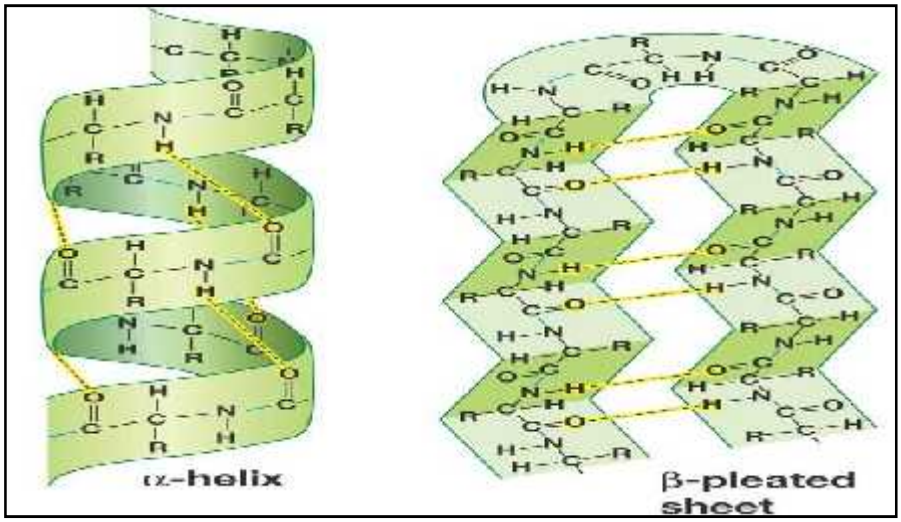

Figure-1.6: α-helical structure of SF formed by intramolecular hydrogen bonds [25].

Due to its amino acid sequence, SF provides opportunities for chemical modification. Polysaccharides are important group that used for modification of silk fibroin properties. Alginate helps to improve the mechanical properties, compressive modulus as well as water absorption of the silk fibroin [15]. Cellulose is used due to it is cheap, biodegradable and moisture absorbent. Silk fibroin blended with cellulose has increased of its mechanical strength since the cellulose enhanced the formation of hydrogen bonds resulted to increase of β-sheet structures [16]. Chitosan used for improving the flexibility or hydrophilic of the silk fibroin while the silk fibroin enhanced the mechanical properties and water insoluble of the chitosan [17]. Mixing with the hyaluronic acid, the compressive modulus of silk fibroin is increased [18].

1.3. Properties of SF

1.3.1 Mechanical Properties

Silk is very sophisticated biomaterial with its significant crystallinity, high elasticity, strength and toughness and resistance to failure in compression. The arrangement of β-sheet crystal, the interphase between the crystals, the semi-crystalline region and the shear alignment of the molecular chains are the mechanical properties of silk. The β-sheet region provides the tensile strength, the semi-crystalline region responsible for the elasticity [6]

1.3.2. Solubility

Crystalline SF is insoluble in solvents such as water. To dissolve SF highly concentrated salt solutions like lithium bromide, calcium chloride should be applied .These electrolyte solutions disturb the hydrogen bonds that stabilize β-sheets. [5-6]

1.3.3. Swelling

The degree of swelling depends on the ionization of the network, its degree of crosslinking and its hydrophilic / hydrophobic balance. Changes in polymer compositions can influence the degree of swelling. [2, 6]

1.3.4. Degradation

Silk will lose its tensile strength within a year. The rate of degradation depends on the tissue implantation site. Silk is considered biodegradable because it is resistant to bacterial and enzymatic degradation [3,6]

1.4 Applications of SF- based materials

Silk is preferable for their strength, low immunogenicity and biocompatibility with other biomaterials used for specific applications in both structural and biological functions.

Hydrogels of SF demonstrated to promote wound healing [4]. Electrospun silk fibers, microspheres, or films or foams were used to support cell adhesion and proliferation of many cells. Silk films are the applications for biocompatible coatings for biomedical implants [14].

Coating biomedical implants with silk films shows potential their surfaces with anticoagulant properties, or inhibit/promote cell adhesion [7].Silk has been also used as anticoagulants for control release application [6].Microspheres coated with silk fibroin have been applied for enzymes, drug and active molecule encapsulations and membrane-permeation controlled [14]

Silk powder can be used for surface coating or treatment of fiber, fillers in films, ink, wound care and enzyme immobilization [5].

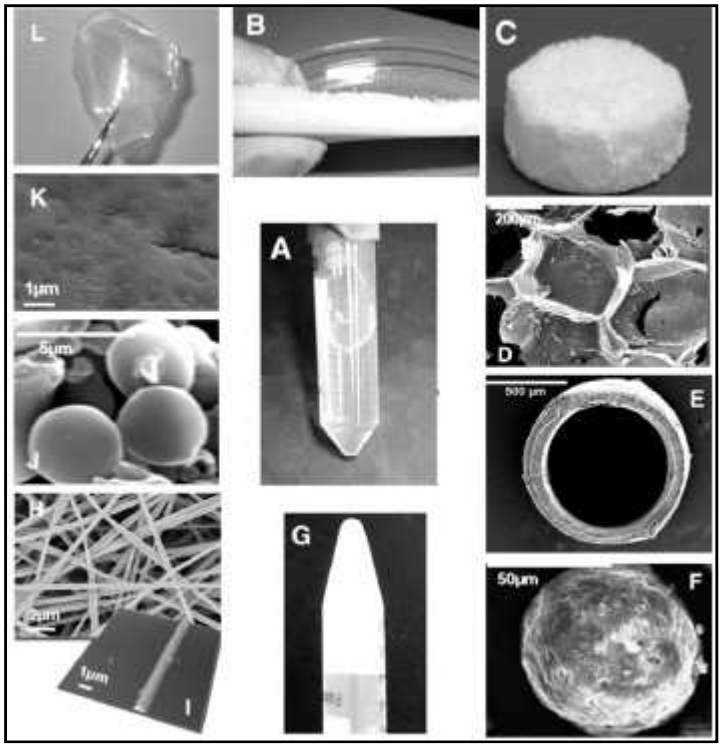

Figure-1.7 Silk-based biomaterials processed from silk solution (A),silk foam (B), silk scaffolds and C), scanning electron microscope image of porous structure of scaffold (D),silk tube(E), microsphere coated with silk layers (F), silk hydrogel (G), silk electrospun fibers (H), atomic fluorescence microscopy image of single electrospun fi bers of silk (I), silk-based microspheres (J), surface of silk films (K), and silk film (L) [13].

1.5. Silk Fibroin Nanoparticles

Nanoparticles may provide advanced biomedical research tools based on polymeric or inorganic formulations or a combination of both. They have the potential to be used in many different biological and medical applications as in diagnostic tests assays for early detection of diseases, to serve as tools for non-invasive imaging and drug development, and to be used as targeted drug delivery systems to minimize secondary systemic negative effects.

Nanoparticles can be prepared from a variety of materials such as protein, polysaccharides and synthetic polymers [20].The choice of materials depends on several factors including

(i) size and morphology of the nanoparticles;

(ii) surface charge and permeability of the nanoparticle;

(iii) degree of biodegradability, biocompatibility and cytotoxicity

1.5.1 Characterization of Nanoparticles

1.5.1.1 Particle Size

The particle sizes are between 1 and 100 nanometers. The nano size of the particles enables conjugation with many molecular markers that can interact at molecular and cellular levels [19].The particle size affects the drug release also. Smaller particles supply larger area [20].That is means that most amount of drug can be loaded to the surface of the particles cause fast drug release. As a drawback, smaller particles tend to aggregate during storage and transportation of nanoparticle dispersion.

1.5.1.2. Particle Stability

Particle stability is an important factor and refers to the potential of measuring the surface charge. Surface charges prevent the agglomeration of nanoparticles polymer dispersions because of strong electrostatic repulsion that increase the stability of the nanoparticles [20].

1.5.1.3. Particle Structure

Nanoparticles are small particles with containing a core and monolayer.For drug delivery applications the multiple polymer layers used to surround the core. In imaging applications that use a basic structure contains an inorganic core and organic monolayer [19].

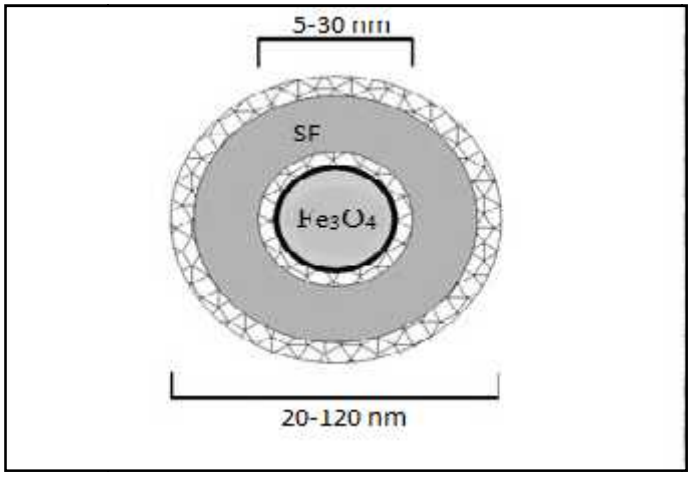

Figure-1.8: Scheme of an iron-oxide nanoparticle. The superparamagnetic Fe_3O_4 core coated by a SF shell.

Protein	Method of fabrication	Particle size (nm)	Remarks
Silk fibroin	Precipitation using water miscible protonic and polar aprotonic organic solvents	35–125	Globular insoluble particles well dispersed and stable in aqueous solution
	Precipitation using water miscible protonic and polar aprotonic organic solvents	50 120	Matrix for immobilization of L-asparaginase
	Microemulsion	167	Color dye doped silk fibroin nanoparticles
	Conjugated covalently with insulin using crosslinking reagent glutaraldehyde	40 120	Insulin silk fibroin nanoparticles bioconjugates
	capillary microdot technique	<100	Sustained and long-term therapeutic delivery of curcumin to breast cancer cells
	Desolvation	150–170	Cellular uptake and control release studies
Silk sericin	Conjugation of sericin with activated PEG	200–400	Overcomes its problem of instability in water and insolubility in organic solvents
	Sericin PEG self assembled through hydrophobic interactions	204	Self assembled nanostructures for immobilization and drug delivery
	Sericin—poly methacrylate core-shell nanoparticles by graft copolymerizing technique	100–150	Potential biomedical application as delivery systems
	Self assembled silk sericin/poloxamer nanoparticles	100 110	Nanocarriers of hydrophobic and hydrophilic drugs for targeted delivery
	Self-assembled silk sericin nanostructures	–	Fractal self-assembly of silk protein sericin

Table -2: Silk Protein nanoparticles, preparation and application [20].

1.5.2. Methods of Fabrication

1.5.2.1. Emulsification

Emulsification occurs on mixing an organic phase and an aqueous phase. This method can be described as the dissolution of hydrophobic substances in an organic solvent which is further emulsified with an aqueous solution at very high shear. After emulsification, the organic solvent removed by evaporation [20].

1.5.2.2 Desolvation

This method involves slow addition of a desolvation factor, such as natural salts or alcohol, to the protein solution. The desolvation factor changes the tertiary structure of protein.At a specific level of desolvation, protein clup will be formed which on crosslinking with a chemical substance results the nanoparticles [19-20]

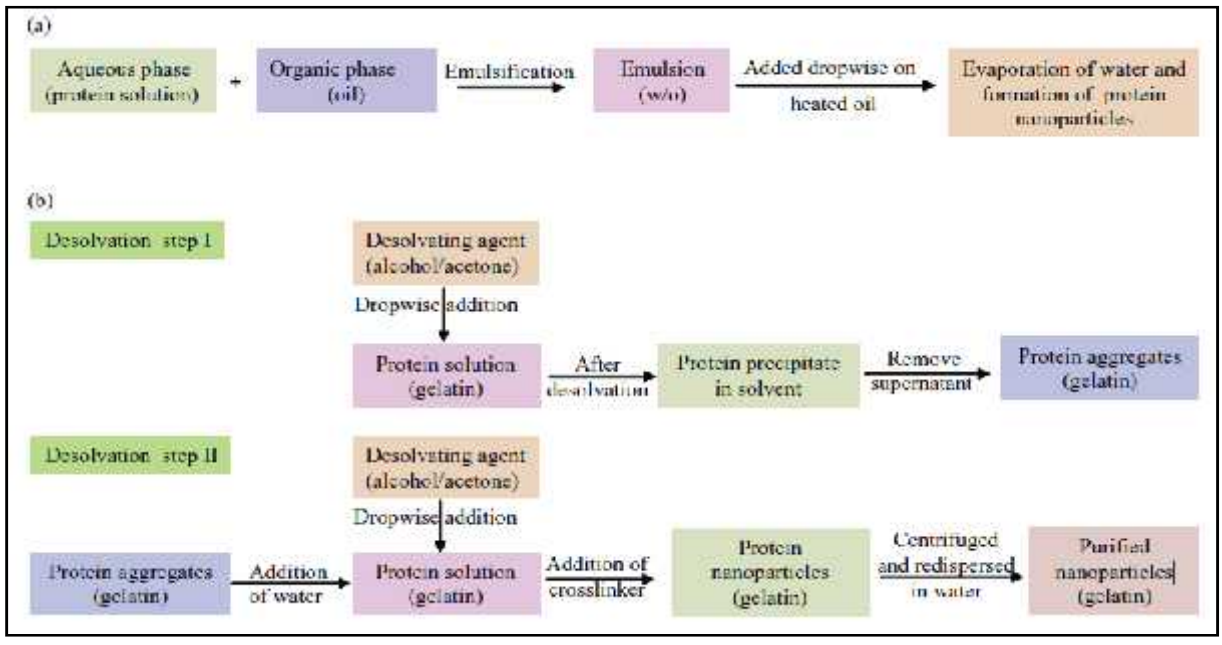

Tablo-3: Schematic representation of nanoparticle preparation. (a) emulsification method, (b) desolvation method [20].

1.5.2.3 Coacervation

The coacervation method is similar to desolvation method,includes mixing of the aqueous protein solution with organic solvent like acetone or ethanol.The difference of coacervation and desolvation method depends on some parameters such as initial protein concentration, temperature, pH, cross linker concentration, the molar ratio of protein/organic solvent and organic solvent adding rate [19-20].

1.5.2.4 Electrospray Drying

The electrospraying method produces relatively monodisperse and biologically active protein particles. This method involves preparation of protein solution by dissolving the dry powder in an electrosprayable solution. Dispersion of the solution followed by solvent evaporation leaves dry residues collected on suitable deposition substrates. Higher production rate of the nanoparticles also increases their size. The biological activity of the electrosprayed protein-based nanoparticles is not affected by the process conditions [19-20]

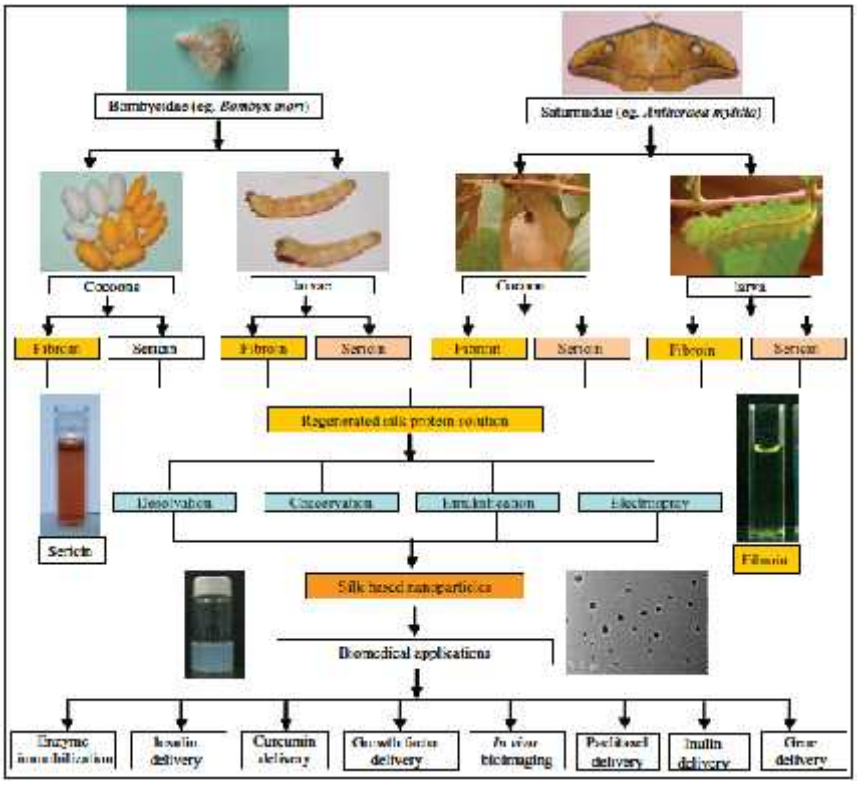

Figure-1.9: Schematic preparation of SF nanoparticles and their biomedical applications [22].

1.6 MRI Imaging Techniques

MRI is a useful problem-solving diagnostic tool in the clinical field because it has higher spatial resolution and contrast in soft tissue than other imaging modalities. MRI is based on the magnetism property of protons that align themselves in a very large magnetic field. These protons originate from water molecules present in our body tissue. A radiofrequency enerated at a particular frequency, known as the “resonance frequency,” can flip the spin of a proton. When the electromagnetic field is turned off, the proton flips back to the original state, generating a radiofrequency signal. This process is called “relaxation.” The receiver coils measure this relaxation, which is turned into an image by a computer algorithm [21].

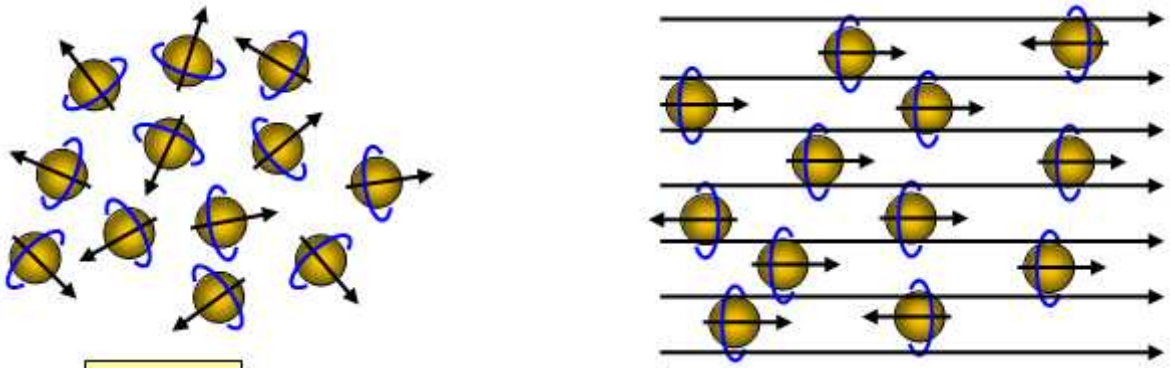

Figure-1.10: Hydrogen protons before and during the magnetic field [26].

MRI contrast agents are used to modify the relaxation rates at time T1 or T2. T1 contrast agents, such as gadolinium, enhance the positive signal on T1-weighted images, while T2 agents, such as Superparamagnetic Iron Oxide Nanoparticle (SPION)-based contrast agents, decrease the signal intensity on T2-weighted images.

1.6.1 Magnetic Properties

In the paramagnetic state, the individual atomic magnetic moments are randomly oriented, and the substance has a zero net magnetic moment if there is no magnetic field. These materials have a relative magnetic permeability greater than one and are attracted to magnetic fields. The magnetic moment drops to zero when the applied field is removed.

But in a ferromagnetic material, all the atomic moments are aligned even without an external field. A ferrimagnetic material is similar to a ferromagnet but has two different types of atoms with opposing magnetic moments. The material has a magnetic moment because the opposing moments have different strengths. If they have the same magnitude, the crystal isantiferromagnetic and possesses no net magnetic moment [22].

Superparamagnetism is refers to the single domain nature of the nanoparticle, which has a net magnetic dipole. In a magnetic field, the magnetic domains of nanoparticles re-orient themselves in a manner similar to paramagnetic materials, but the magnetic moment of nanoparticles will be much higher than that of paramagnetic substances. In the absence of a magnetic field, the dipole randomly orients with zero magnetic moment. Due to this property, SPION have less chance of aggregation. The function of SPION in MRI contrast enhancement is attributed to their ability to change the nuclear spin relaxation of water protons and cause the region of interest to darken [21].

1.6.2 Nanoparticles as Contrast Agents

A contrast agent is a substance used to enhance the contrast of structures or fluids within the body in medical imaging.

Magnetic nanoparticles (MNP) are composed of ferromagnetic elements such as iron, cobalt, nickel, or their oxides and alloys. MNPs made of iron oxide (magnetite Fe_3O_4 or magnemite Fe_2O_3) and gadolinium used as contrast agents in MRI for biological applications due to their ability to dissociate into iron and oxygen inside the body, which can safely be eliminated and utilized in metabolic and oxygen transport systems [17].

SPION are used as an MRI contrast agent because the T2 relaxivity of a SPION-based agent is much higher than that of gadolinium agents. The physiochemical properties of SPION, such as charge, size, and surface chemistry, can influence biodistribution, stability, and metabolism. By giving proper surface coating that are biocompatible and biodegradable, SPION can avoid immune response and serum protein adsorption. Surface charge is a major factor in determining the colloidal nature of nanoparticles, and it can change size of nanoparticles by aggregation. Hence neutral surfaces are more biocompatible than charged surfaces [21].

A typical SPION is composed of magnetite (Fe_3O_4) or maghemite (Fe_2O_3), with appropriate coatings to maintain aqueous stability. The SPION are synthesized by a wide range of methods,including co-precipitation, thermal decomposition, and microemulsion. Thermal decomposition for the synthesis of SPION is generally more popular as the nanoparticles obtained this way possess high crystallinity, high magnetization, and distribution. As the nanoparticles are hydrophobic, which is required to provide appropriate coating for biomedical application. The co-precipitation method is the most commonly accepted method for synthesizing SPION. It involves the addition of a concentrated base to divalent or trivalent ferrous salt solutions. The microemulsion technique has the advantage of controlling the size of nanoparticles by acting as a nano-reactor. This technique involves the formation of SPION either by water-in-oil or oil-in-water emulsion.

Method	Parameters	Reaction temperature (°C)	Reaction time	Solvent	Size (nm)	Yield
Thermal decomposition	Nitrogen atmosphere, reflux condition	100–320	Slow	Water	1.5–8	High
Co-precipitation	Ambient condition	20–90	Fast	Organic	2–15	High
Microemulsion	Ambient condition	20–50	Fast	Organic	2–12	Low

Table-4: Comparison of synthesis methods of magnetic nanoparticles [22].

2. EXPERIMENTAL

2.1. Materials

Bombyx mori silkworm cocoons were supplied by North Cyprus villages. Sodium carbonate (Na_2CO_3), Calcium chloride ($CaCl_2$), Iron (III) oxide, Methanol (CH_3OH), Sodium chloride (NaCl), Potassium chloride (KCl), Hydrochloric acid (HCl), Sodium hydroxide (NaOH), di-Sodium hydrogen phospahate dehydrate ($Na_2HPO_4.2H_2O$), Potassium dihydrogen phosphate (KH_2PO_4), Ethanol (C_2H_5OH) and Acetic acıd (CH_3COOH) were purchased from E.Merck D-6100 Darmstadt.Sodium triphosphate pentabasic (TPP) was purchased from Sigma-Aldrich (St.Louis, MO, USA). Glyserine was purchased from pharmacy. Ultrapure water-obtained from Near East University Medicine Faculty-was used in all step to get silk fibroin.

2.2. Methods

2.2.1. Preparation of Sodium Carbonate Solution

2.12 g of Na_2CO_3 is stirred with 200 ml of pure water to get 0.1 M Na_2CO_3 solution to be used in degumming process.

2.2.2 Preparation of TPP solution

To get 0.1 M TPP solution, 7.36 g TPP is stirred with 200 ml of pure water. It is used in nanoparticle preparation process to make physical cross-linking.

2.2.3. Preparation of PBS

Although there are different ways to prepare PBS, we used the following constituents:

Salt	Concentration	Concentration
(—)	(mmol/L)	(g/L)
NaCl	137	8.01
KCl	2.7	0.2
$Na_2HPO_4.2\ H_2O$	10	1.78
KH_2PO_4	2.0	0.27
pH	7.4	7.4

Table-5: Phosphate Buffer Saline Contents

After preparing the PBS solution the pH is adjusted to 7.4 by adding either HCl or NaOH depending on the pH value when it was above or below 7.4.

2.2.4. Preparation of Acetic Acid Solution

For 0.5 M acetic acid solution, 5.72 ml pure glacial acetic acid was diluted by pure water to 200 ml. After that the pH is adjusted to1.2 by HCl or NaOH in order to pH value was above or below 1.2.

2.2.5. Purification of Silk Fibroin

2.2.5.1. Degumming

Degumming is the process of removal and separation of the gum-like sericin protein from the silkworm silk. In this process, firstly the Bombyx mori cocoons were cut into small pieces and measured 0.9998 -1.0003 g and boiled for 3 hour in a aqueous solution of 0.1 M Na_2CO_3, at 70 ^oC on a magnetic stirrer at the speed of 1 rpm. Then the degummed silks are washed and rinsed thoroughly with pure water to get rid of the gum-like sericin protein. This procedure is continued three times and then they were dried at room temperature to obtain silk fibers.

Figure-2.1: Degumming process

Figure- 2.2: Degummed Silk Fibers

2.2.5.2. Dissolution of Degummed Silk Fibers

Dissolution is the process of dissolving the silk fibers to have an aqueous form of silk fibroin, the main principle is breaking down the long polypeptide chains into shorter chain lengths to get the aqueous solution.This process is mixing the solution of $CaCl_2$, C_2H_5OH, H_2O (1:2:8 mole ratio) and degummed silk fibers, at 75^oC with continuous stirring until total dissolution.

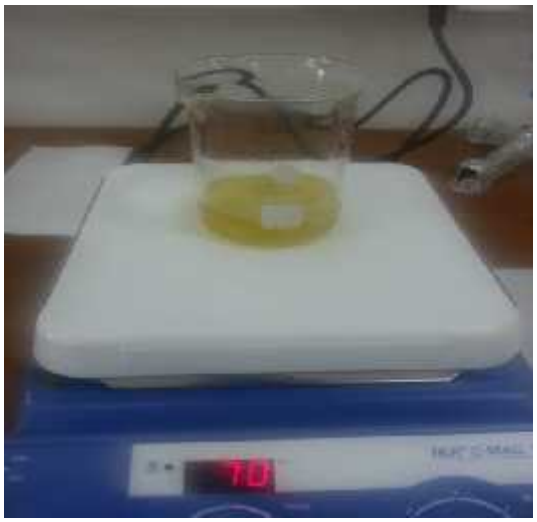

Figure- 2.3: Silk fibers dissolving in the electrolyte solution

2.2.5.3. Dialysis

Dialysis is removal of the ions within the solution obtained from the dissolution step. Electrolyte solution was dialyzed continuously for 72 h against running ultrapure water to remove ions using a cellulose semi-permeable membrane (made of Carboxymethyl, diameter: 2.7 cm).The liquid silk fibroin was stored to be used in nanoparticle preparation.

Figure-2.4: Dialysis System

2.2.6. Preparation of Silk Fibroin Nanoparticles

0.1 M TPP is used as a physical cross-linking environment for nanoparticles. Into 20 ml of TPP, 3 ml SF was dropped helped by a syringe to create nanostructures. Another sample is created by adding 1 ml Fe_2O_3-dissolved in concentrated HCl-solution for trying to obtain nanoparticles as contrast material for imaging techniques. After this process, waited one day and the beads were created.

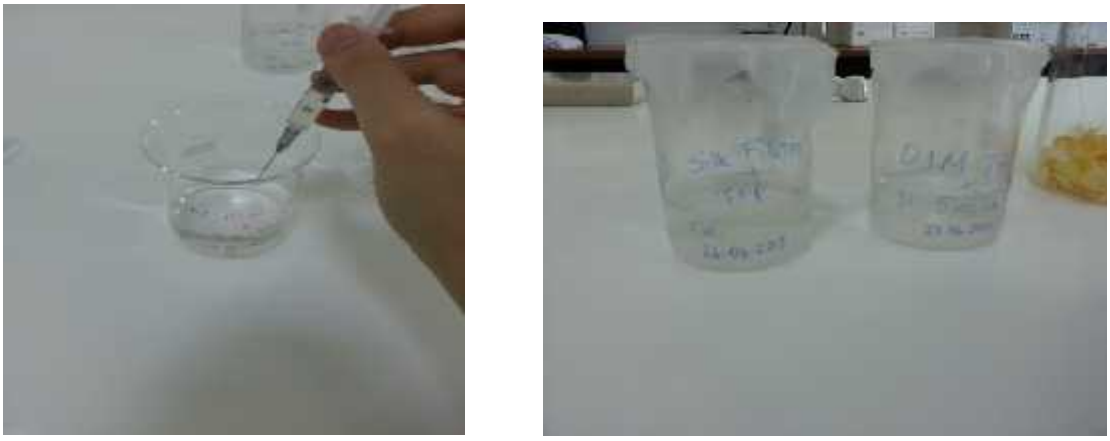

Figure-2.5: Preparation of Silk Fibroin Nanoparticles

2.2.7. Preparation of Silk Fibroin- Iron (III) oxide Biofilms

Silk fibroin films were prepared by the mixing of 2 ml of silk fibroin, 0.0563 g glycerine and 50µl Fe solution. Then the solution was placed on to smooth lams at room temperature and constant humidity. After one day, dried with methanol to improve β-sheet crystallinity. The silk films were washed with ultra pure water to remove methanol.

3. RESULTS AND DISCUSSION

3.1. Creating Silk Fibroin and Silk Fibroin-Iron Nanoparticles

The aqueous SF was obtained 6% w/v SF/ ($CaCl_2$: H_2O: C_2H_5OH) electrolyte solution. During the dialysis process the exact content of SF decreased to half of the original due to water absorption of aqueous silk fibroin solution.

Iron (III) oxide is insoluble in neither in water nor organic solvent. It can be dissolved in concentrated acids. That is why concentrated hydrochloric acid (HCl) is used to dissolve iron (III) oxide.

Time	Fe^{+3}	TPP volume	SF volume	SF concentration
5 min	-	20 ml	3 ml	6 %
15 min				
30 min				
60 min				
24 h				
5 min	1 ml			
15 min				
30 min				
60 min				
24 h				

Table-6: List of samples

Five samples were collected from each solution at different time intervals and their particle sizes and shapes are detected under the electron microscope.

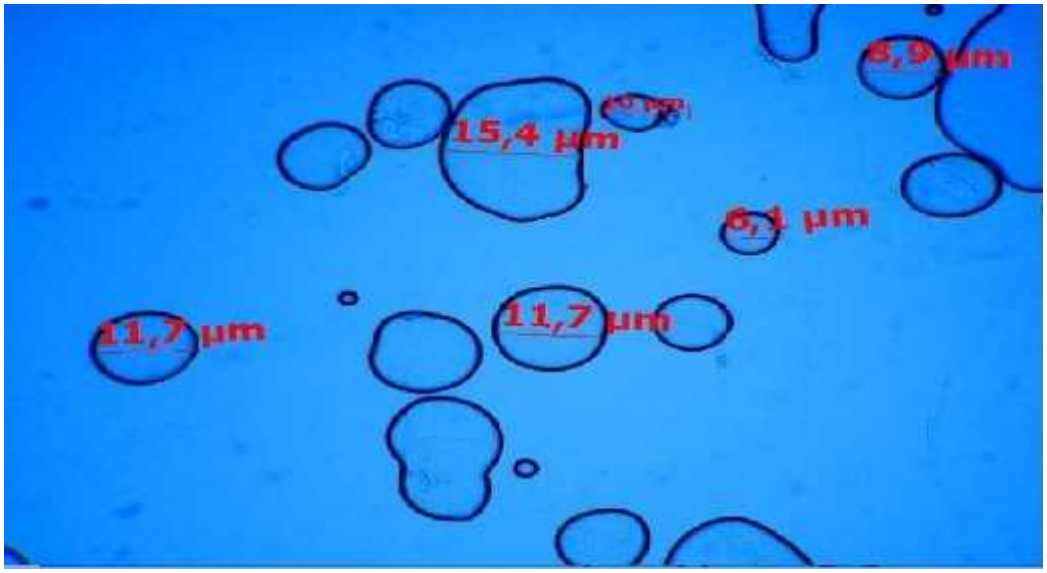

Figure-3.1.: Normal SF drops after 5 minutes

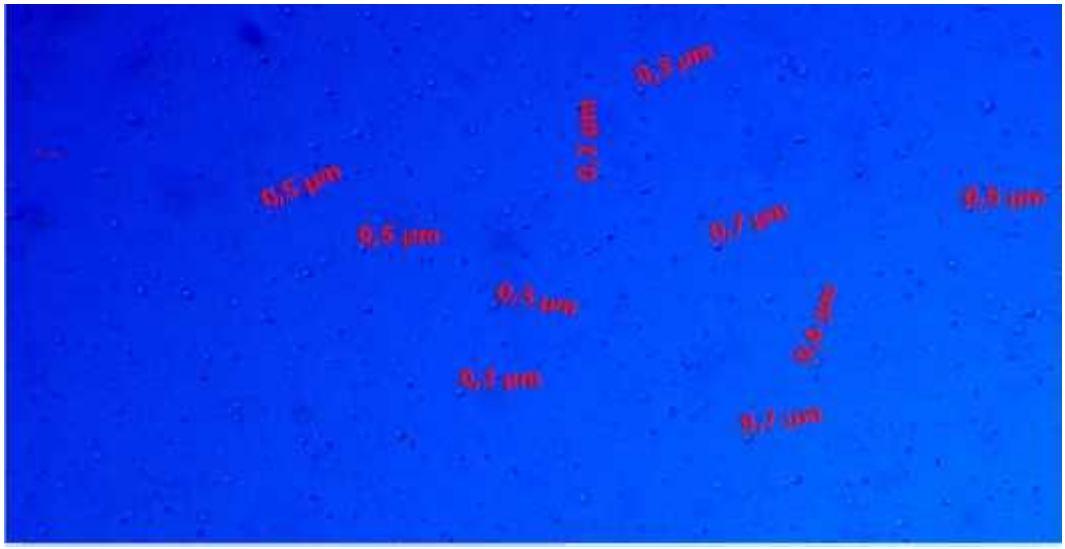

Figure-3.2: Normal SF spheres after 15 minutes

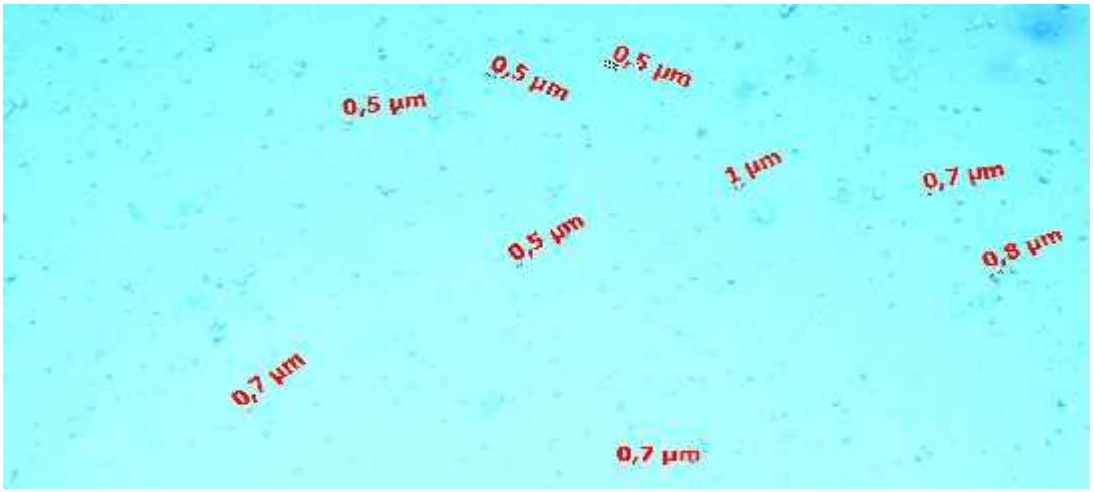

Figure-3.3: Normal SF spheres after 30 mins

Figure-3.4: Normal SF spheres after 60 mins

Figure-3.5.: Normal SF spheres after 24 hours

1.	9.65	6.	11.7	11.	7.93
2.	8.43	7.	15.4	12.	5.75
3.	11.32	8.	1.66	13.	8.83
4.	18.41	9.	1.85	14.	9.78
5.	10.67	10.	9.46	15.	6.58

Table -7: Randomly selected 15 SF particles with average diameter 9.16µm and standard deviation 19.195 µm in 232.63 cm^2 (17.65 cm x 13.18 cm) area after 5 minutes

1.	0.5	11.	0.06	21.	0.3	31.	0.2	41.	0.1
2.	0.3	12.	0.2	22.	0.2	32.	0.16	42.	0.16
3.	0.5	13.	0.1	23.	0.1	33.	0.08	43.	0.16
4.	0.3	14.	0.16	24.	0.16	34.	0.1	44.	0.1
5.	0.27	15.	0.06	25.	0.2	35.	0.16	45.	0.1
6.	0.16	16.	0.3	26.	0.1	36.	0.2	46.	0.06
7.	0.1	17.	0.1	27.	0.1	37.	0.2	47.	0.04
8.	0.06	18.	0.16	28.	0.16	38.	0.1	48.	0.04
9.	0.2	19.	0.1	29.	0.1	39.	0.06	49.	0.04
10.	0.16	20.	0.1	30.	0.2	40.	0.27	50.	0.06

Table -8: Randomly selected 50 SF particles with average diameter 0.158µm and standard deviation 0.0104 µm in 218.51 cm^2 (17.65 x 12.38) area after 15 minutes

1.	0.7	11.	0.07	21.	0.07	31.	0.48	41.	0.18
2.	0.96	12.	0.07	22.	0.07	32.	0.07	42.	0.29
3.	0.77	13.	0.07	23.	0.11	33.	0.4	43.	0.17
4.	0.59	14.	0.18	24.	0.77	34.	0.17	44.	0.17
5.	0.29	15.	0.4	25.	0.59	35.	0.17	45.	0.4
6.	0.29	16.	0.29	26.	0.7	36.	0.18	46.	0.18
7.	0.4	17.	0.29	27.	0.21	37.	0.11	47.	0.11
8.	0.07	18.	0.05	28.	0.29	38.	0.07	48.	0.17
9.	0.07	19.	0.11	29.	0.29	39.	0.07	49.	0.07
10.	0.07	20.	0.11	30.	0.11	40.	0.17	50.	0.07

Table- 9: Randomly selected 50 SF particles with average diameter 0.25µm and standard deviation 0.05 µm in 296.55 cm^2 (22.23 x 13.34) area after 30 minutes

1.	0.5	11.	0.5	21.	0.6	31.	0.3	41.	0.3
2.	0.8	12.	0.8	22.	0.4	32.	0.3	42.	0.2
3.	0.8	13.	1.1	23.	0.3	33.	0.2	43.	0.3
4.	1.1	14.	0.5	24.	0.2	34.	0.2	44.	0.2
5.	1.1	15.	0.3	25.	0.5	35.	0.3	45.	0.4
6.	1.1	16.	0.2	26.	0.8	36.	0.4	46.	0.6
7.	0.8	17.	0.4	27.	1.1	37.	0.5	47.	0.5
8.	0.5	18.	0.5	28.	1.3	38.	0.6	48.	0.3
9.	0.3	19.	0.8	29.	0.8	39.	0.4	49.	0.8
10.	0.8	20.	0.6	30.	0.5	40.	0.8	50.	1.1

Table-10: Randomly selected 50 SF particles with average diameter 0.574µm and standard deviation 0.09 µm in 427.03 cm^2 (26.54 x16.09) area after 60 minutes

1.	0.8	11.	1.1	21.	0.5
2.	0.5	12.	0.8	22.	0.4
3.	0.5	13.	0.5	23.	0.3
4.	0.8	14.	0.5	24.	0.4
5.	0.8	15.	0.3	25.	0.3
6.	1.1	16.	0.5	26.	0.5
7.	0.5	17.	0.8	27.	0.3
8.	0.5	18.	0.8	28.	0.4
9.	0.5	19.	0.5	29.	0.4
10.	0.8	20.	0.8	30.	0.3

Table-11: Randomly selected 30 SF particles with average diameter 0.573µm and in standard deviation 0.052 µm in 434.6 cm^2 (26.5 x 16.4) area after 24 hours

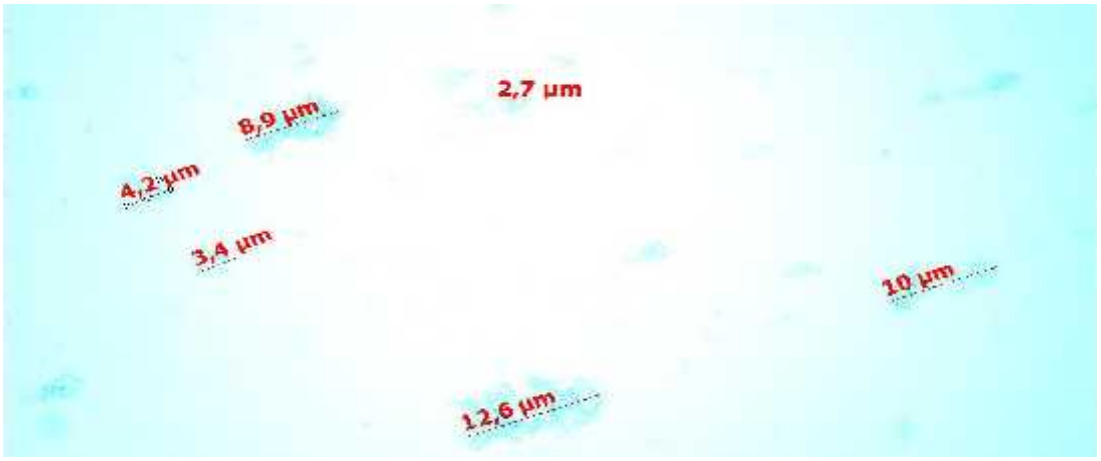

Figure-3.6: Fe^{+3} added SF particles after 5 minutes

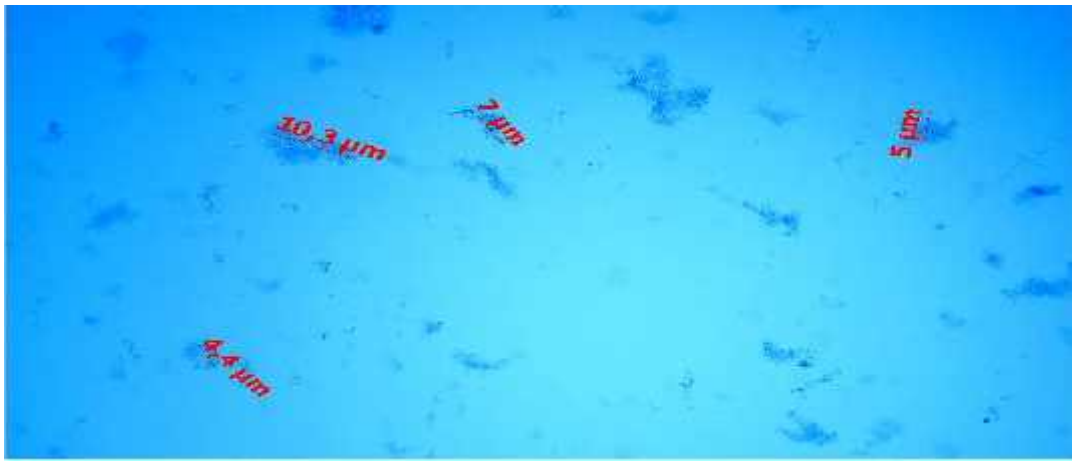

Figure-3.7: Fe^{+3} added SF particles after 15 minutes

Figure-3.8: Fe^{+2} added SF particles after 30 minutes

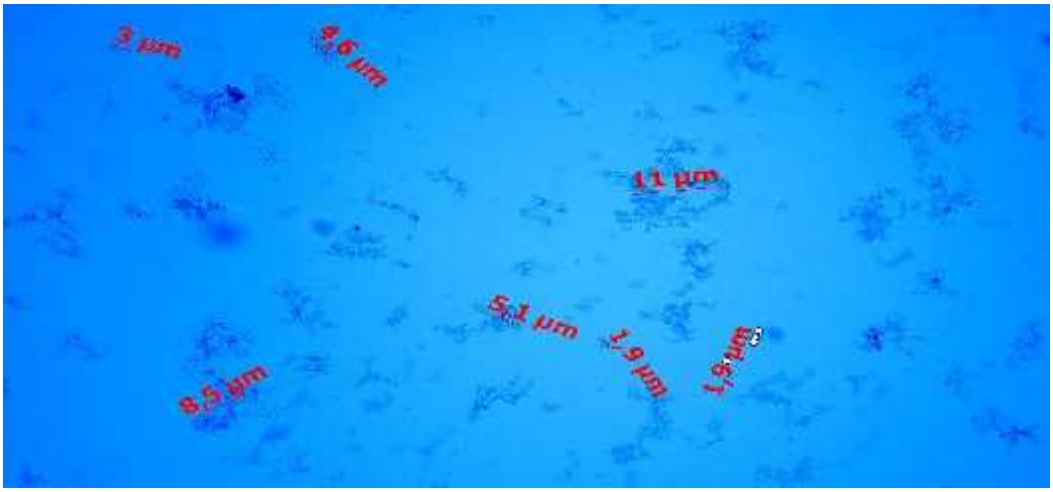

Figure-3.9: Fe^{+3} added SF particles after 60 minutes

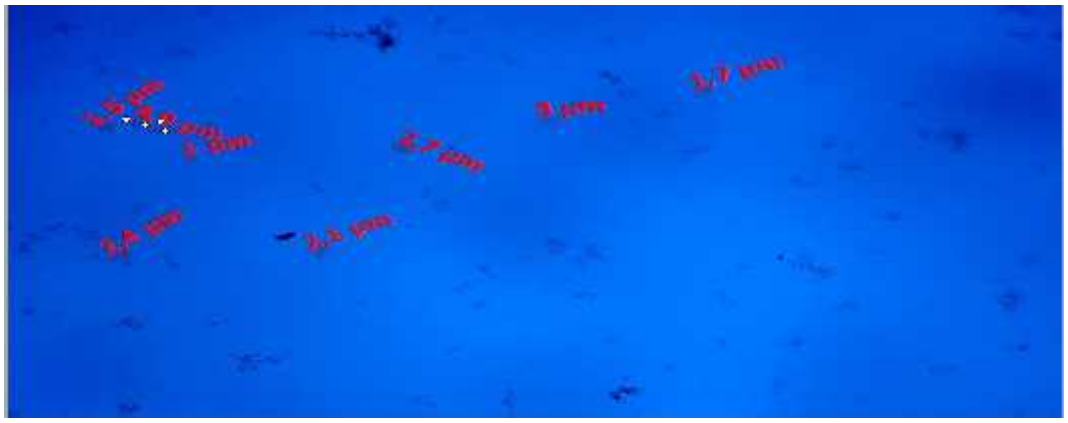

Figure-3.10: Fe^{+3} added SF particles after 24 hours

1.	4.2	6.	12.3	11.	3.03
2.	3.18	7.	8.19	12.	1.44
3.	8.9	8.	1.92	13.	2.94
4.	2.55	9.	5.64	14.	2.31
5.	10.17	10.	1.74	15.	2.46

Table-12: Randomly selected 15 SF and Fe^{+3} particles with average diameter 4.7 µm and Standard deviation 12.09 µm in 503.22 cm^2(15.77x31.91) area after 5 minutes

1.	5.26	6.	1.56	11.	13.91
2.	4.4	7.	3.44	12.	1.83
3.	12.08	8.	5.42	13.	2.26
4.	6.55	9.	1.83	14.	6.39
5.	1.72	10.	3.28	15.	3.11

Table-13: Randomly selected 15 SF and Fe^{+2} particles with average diameter 4.87 µm and Standard deviation 13.85 µm in 443.25 cm^2(16.67x26.59) area after 15 minutes

1.	6.2	6.	2.38	11.	4.62
2.	3.19	7.	1.53	12.	8.23
3.	2.38	8.	2.25	13.	4.85
4.	6.87	9.	3.19	14.	1.53
5.	2.51	10.	8.89	15.	9.25

Table-14: Randomly selected 15 SF and Fe^{+2} particles with average diameter 4.52 µm and Standard deviation 7.38 µm in 433.72 cm^2(16.51x26.27) area after 30 minutes

1.	1.9	6.	9.92	11.	1.72
2.	9.27	7.	1.73	12.	6.29
3.	6.5	8.	3.15	13.	2.49
4.	2.85	9.	2.67	14.	7.54
5.	1.9	10.	2.38	15.	1.54

Table-15: Randomly selected 15 SF and Fe^{+2} particles with average diameter 4.123 µm and Standard deviation 8.60µm in 431.31 cm^2 (16.35x26.38) area after 60 minutes

1.	1.86	6.	0.98	11.	1.58
2.	2.1	7.	3.22	12.	0.98
3.	2.47	8.	1.22	13.	2.7
4.	0.98	9.	1.58	14.	1.35
5.	2.47	10.	1.35	15.	1.72

Table-16: Randomly selected 15 SF and Fe^{+2} particles with average diameter 1.77 µm and Standard deviation 0.47µm in 435.88 cm^2 (16.43x26.53) area after 24 hours

It can be seen that the particles of normal SF are spherical without apparent aggregation or adhesion at the beginning. This was caused by the amphiphilic property of silk fibroin in the aqueous TPP environment.

Particle sizes show that the SF particles were quite homogeneous varied from 0.04µm-1.1µm. It can be seen that the particle size is getting smaller and the particles started to have a chain structure due to passed time.

The Fe^{+3} added SF particles could not have the regular spherical structure. That is why the concentrated HCl that is used to dissolve iron (III) oxide most probably increases the acidity level of SF and damage the SF morphology. Instead of not being in uniform shape, the particle size was getting smaller after a day.

3.2. Creating Silk Fibroin and Silk Fibroin-Iron Biofilms

One biofilm sample created by SF and Glys.Glys was added in order to increase the elasticity of biofilms for the purpose of being control group of biofilm experiments. For the other samples Fe solution was added.

After the biofilms were created they were examined for their swelling properties in the PBS and ABS solutions.

The swelling ratios were calculated by using:

$$Swelling\ \% = \frac{weight\ x\ - weight(dry)}{weight(dry)} \times 100\ \% \qquad \text{Eq (1)}$$

Where weight(x) is the pieces of biofilms that measured at any given time and the weight(dry) is the weight of the biofilm pieces in their dry state.

3.2.1. Swelling Test for SF based biofilms in PBS solution at pH7.4

Biofilms	**Proportions**	**Weight in dry state**
SF+Glys	2mL+0.0563gr	0.0073 g
SF+Glys+Fe_2O_3	2mL+0,0563 gr+50µL	0.0058 g

Table-17: Properties of SF, SF and Fe biofilms which were used in PBS swelling test

Time (Minutes)	SF+Glys Weight(g)	SF + Glys + Fe_2O_3 Weight(g)
5	0.0119	0.0031
10	0.0119	0.0026
15	0.0124	0.0031
20	0.0131	0.0031
25	0.0114	0.0022
40	0.0128	0.0025
55	0.0121	0.0022
70	0.0120	0.0017
85	0.0115	0.0011
115	0.0123	0.0007
175	0.0127	0.0009
235	0.0119	0.0010
295	0.0117	0.0011
1735	0.0126	0.0016
3175	0.0127	0.0005

Table-18: The weight results of Sf, SF and Fe biofilms in PBS at pH 7.4

The swelling ratios of the measured values in Table18 can be calculated by applying Eq (1)

Time (Minutes)	SF+Glys (%)	SF + Glys + Fe_2O_3 (%)
5	63.01	47.62
10	63.01	23.80
15	69.86	47.62
20	79.45	47.62
25	56.16	4.76
40	75.34	19.04
55	65.75	4.76
70	64.38	-19.04
85	57.53	-47.62
115	68.49	-66.67
175	73.97	-57.38
235	63.01	-52.38
295	60.27	-47.62
1735	72.60	-71.43
3175	73.97	-76.19

Table-19: The swelling ratios of SF, SF and Fe biofilms in PBS at pH 7.4

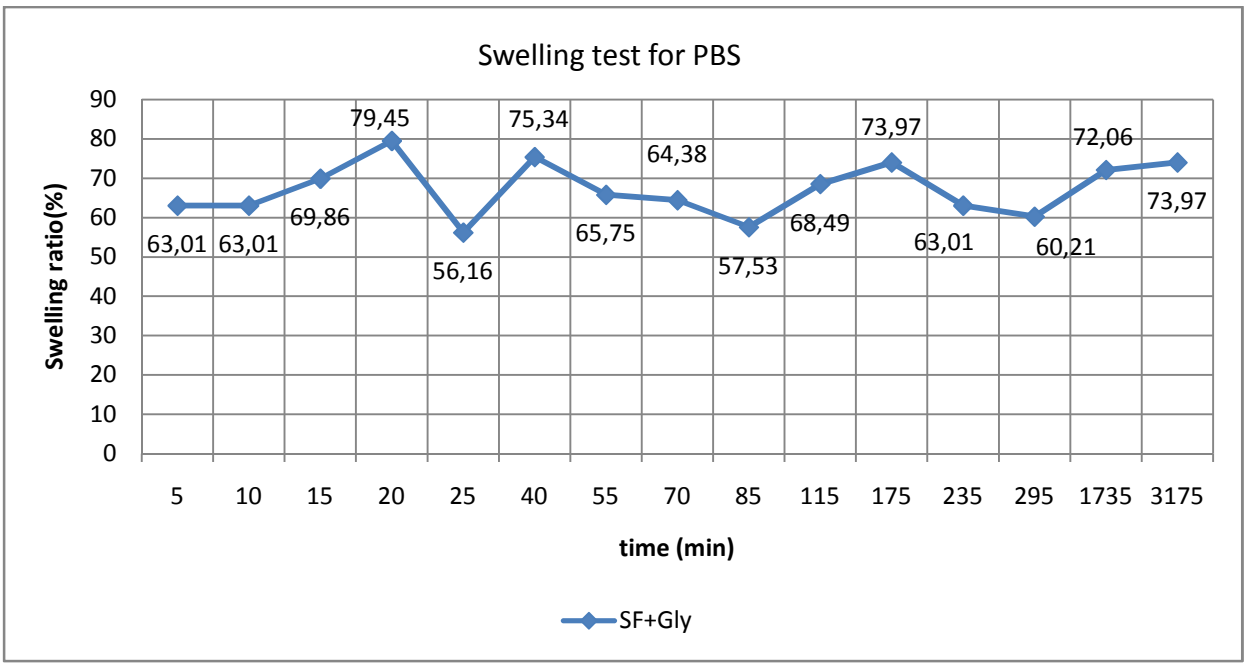

Figure-3.11: Swelling ratios of SF biofilms in PBS at pH 7.4

In the Figure 3.11, firstly the swelling ratio remains stable than begins increasing to the maximum value. After 20 minutes the swelling potential starts to decrease and increase that states the SF biofilms swell and collapse at the basic pH 7.4

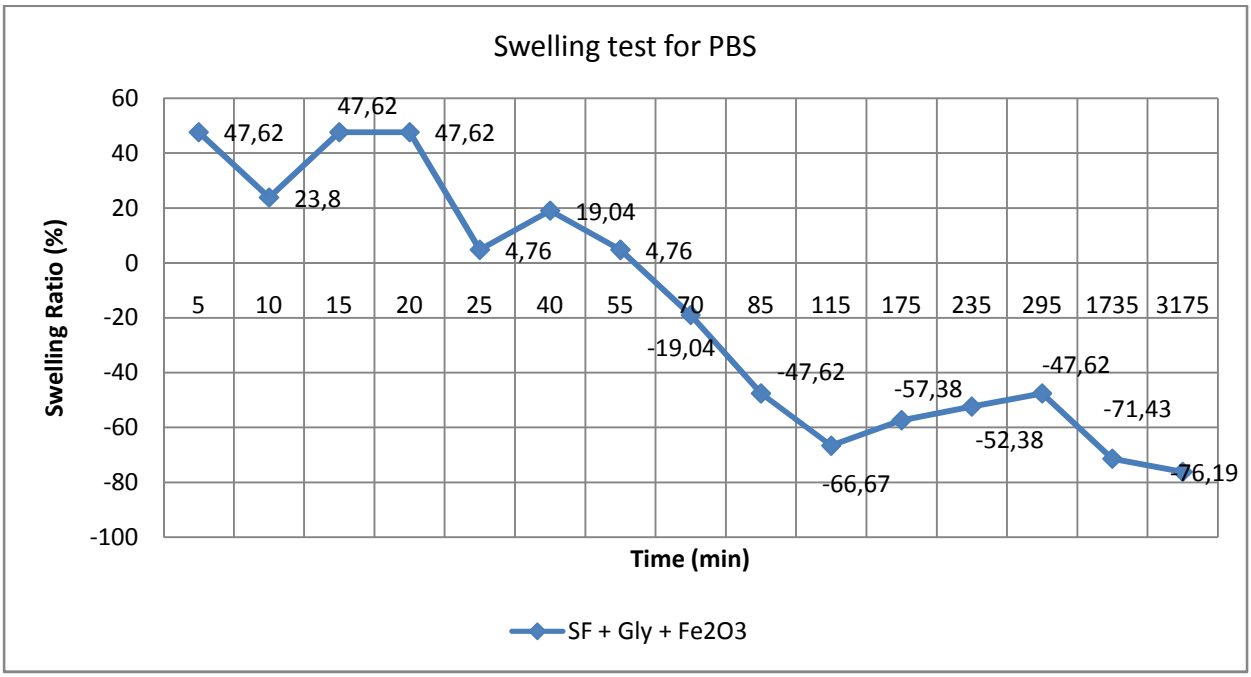

Figure-3.12: Swelling ratios of SF and Fe biofilms in PBS at pH 7.

The Figure 3.12 represents the behaviour of SF and Fe_2O_3 biofilms at the basic pH. As seen in the graphic, firstly swelling potential remains stable than starts to decrease. This decreasing can be caused from the decomposition of the films in the basic environment.

3.2.2. Swelling Test for SF based biofilms in ABS solution at pH 1.2

Biofilms	Proportions	Weight in dry state
SF+Glys	2mL+0.0563g	0.0097 g
SF+Glys+Fe_2O_3	2mL+0,0563 gr+50µL	0.0011 g

Table-20: Properties of SF, SF and Fe biofilms which were used in ABS swelling test

Time (minutes)	SF+Glys Weight (g)	SF+Glys+Fe_2O_3 Weight (g)
5	0.0154	0.0017
10	0.0153	0.0019
15	0.0197	0.0013
20	0.0164	0.0014
25	0.0174	0.0016
40	0.0150	0.0006
55	0.0156	0.0012
70	0.0143	0.0008
130	0.0150	0.0006
190	0.0165	0.0004
250	0.0166	0.0005
1690	0.148	0.0007
3130	0.0140	0.0004

Table-21: The weight results of SF, SF and Fe biofilms in ABS at pH 1.2

The swelling ratios of the measured values in Table21 can be calculated by applying Eq. (1)

Time(minutes)	SF+Glys (%)	SF+Glys+Fe_2O_3(%)
5	58.76	54.54
10	57.73	72.72
15	103.09	18.18
20	69.07	27.27
25	79.38	45.45
40	54.64	-45.45
55	60.82	9.09
70	47.42	-27.27
130	54.64	-45.45
190	70.10	-63.63
250	71.13	-54.54
1690	52.58	-36.36
3130	44.32	-63.63

Table-22: The swelling ratios of SF,SF and Fe biofilms in PBS at pH 1.2

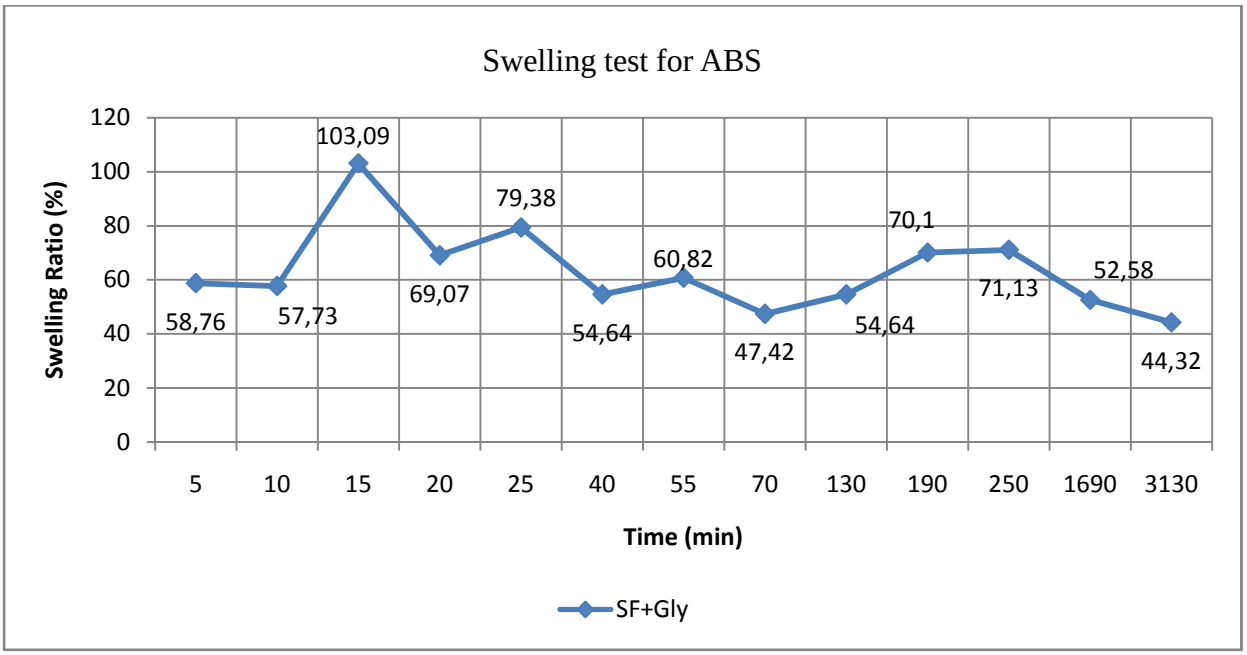

Figure-3.13: Swelling ratios of SF biofilms in ABS at pH 1.2

Figure-3.13 shows the swelling potential of SF biofilms at the acidic pH. The swelling ratio decreases a little at first then begins to increase to the maximum value and decrease again. This shows the SF biofilms swell and collapse continuously in the acidic circumstances.

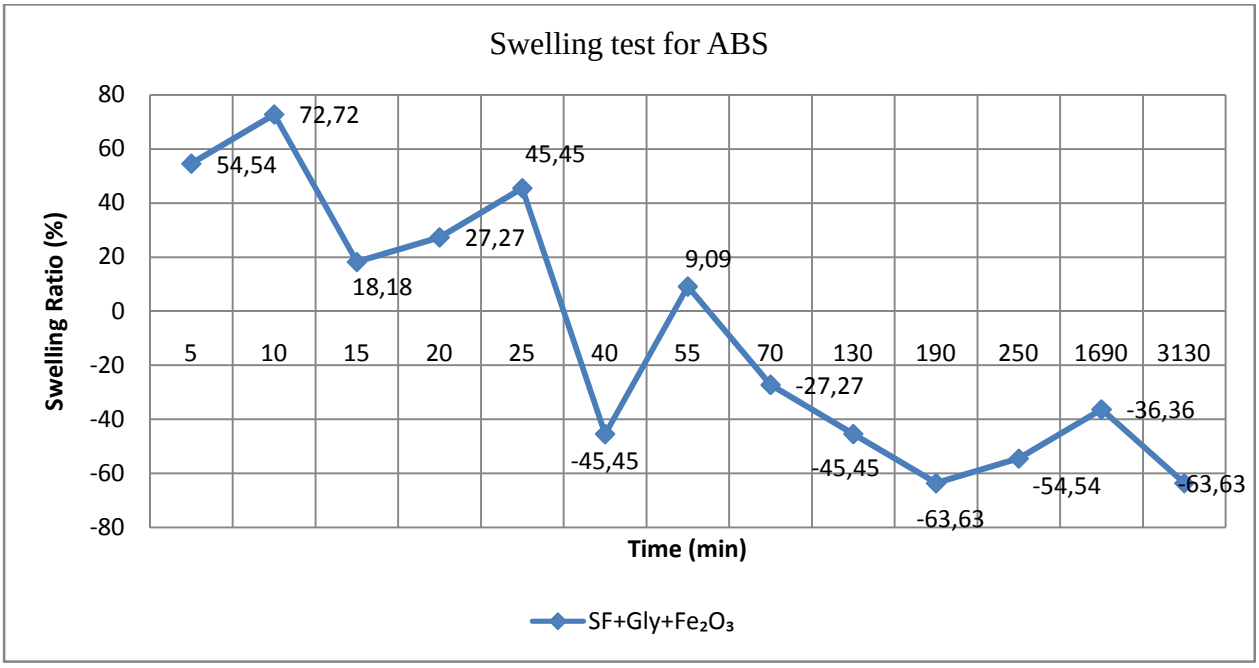

Figure-3.14: Swelling ratios of SF and Fe biofilms in ABS at pH 1.2

This graphic represents the acidic behaviour of SF and Fe_2O_3 biofilms. It can be seen from the graphic the swelling ratio of biofilm increases to the maximum value after 10 minutes. Then stars to decrease and increase as the films swell and collapse. After 70 minutes the Fe_2O_3 contained biofilm has negative swelling ratio as a result of losing in weight in order to be breaking down and starting to dissolve in the acidic environment.

3.3. Antimicrobial Activity

Antimicrobial activity is the sensitivity of bacteria to the antibiotics. The antimicrobial activity of a material based on the behaviour of allowing or inhibiting the bacterial growth. Although there are different methods to test the antimicrobial activity, in this experiment the Kirby-Bauer method which is based on the diffusion of antibiotics through a small disc.

This method states that if a material has antimicrobial effect, it kills the bacteria and a clear ring called zone of inhibition occurs around the disc as shown in the Figure 3.15.

Figure-3.15: Positive-negative control of bacterial test

In the antimicrobial activity experiments, firstly agar was poured into the petri dishes to supply the microbiological growth medium at the pH level 7.2-7.4. Then 100 µl E.coli bacteria were added to medium. The disc was placed in the middle of the medium then the samples were applied to disc to be diffused. Only liquid SF was applied to disc, however the SF particles and SF biofilms were put in the medium without disc. Then samples incubated overnight at 37^{o}C.

Figure-3.16: SF biofilms

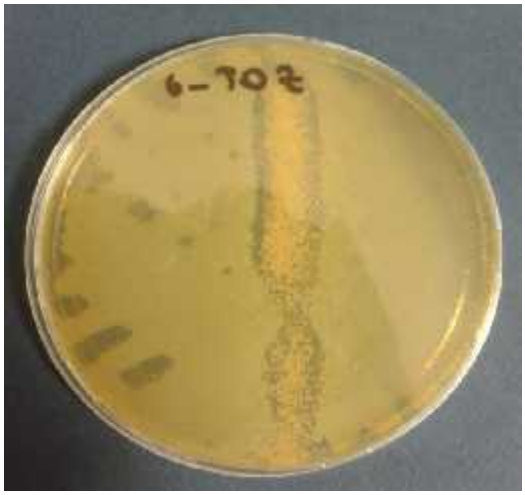

Figure-3.17: SF particles

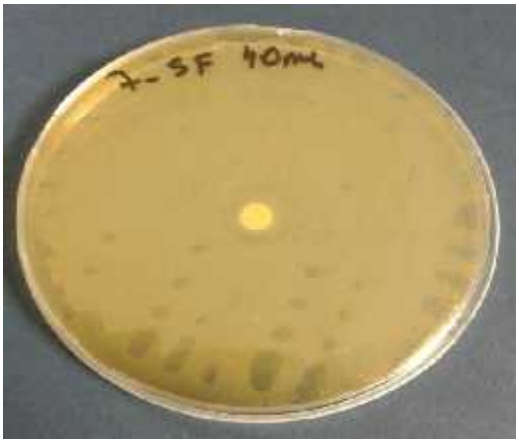

Figure-3.18: Liquid SF 40µl

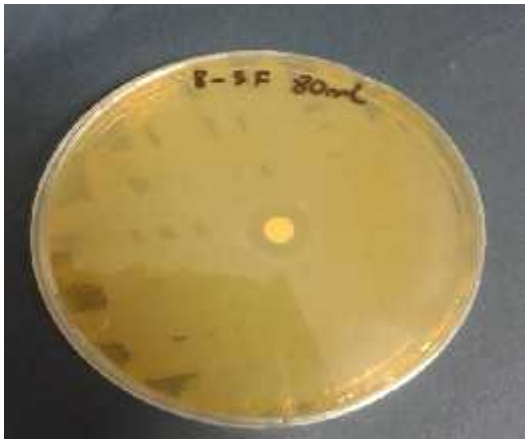

Figure-3.19: Liquid SF 80µl

The experiments prove that silk fibroin has bactericidal property which is mean have bacteria killing behaviour. The effect of bacteria killing is increased as the amount of SF is increased.

The SF particles have also bactericidal behaviour. There was a clear zone around the particles. However, the SF biofilm has no bactericidal property but has bacteriostatic behaviour that is preventing the bacteria from growing so the immune system can overcome bacteria.

4. CONCLUSION

Silk fibroin is a versatile biomaterial that can be prepared in various forms and shapes. The biocompatibility, biodegradability and the mechanical properties of silk fibroin are the important factors for selecting as biomaterial.

In this study silk fibroin based biomaterials were created such as nanoparticles and biofilms include iron ion. Beside the dimentions and the antimicrobial activity of particles, the swelling potential of the biofilms were also be examined.

- Nanoparticle size plays a critical role in maintaining the magnetic properties and the rate of internalization by the target cells. An optimum nanoparticle size should be between 10 to 100 nm to prevent the removal of nanoparticles from circulation and enables them to pass through small capillaries.
- However, in our experiments the particle sizes show that the SF particles were quite homogeneous varied from 0.04µm- 1.1µm. It can be seen that the particle size is getting smaller and the particles started to have a chain structure due to passed time.
- The Fe^{+3} added SF particles could not have the regular spherical structure. That is why the concentrated HCl that is used to dissolve iron (III) oxide most probably increases the acidity level of SF and damage the SF morphology. Instead of not being in uniform shape, the particle size was getting smaller after a day.
- From the swelling test graphics and observations of the silk fibroin, silk fibroin iron (III) oxide biofilms. Generally it can be said that silk fibroin biofilms behave like an intelligent biomaterial by swelling and collapsing in both acidic and basic circumstances.
- By the graphics and the measurements of silk fibroin iron (III) oxide biofilms, it observed that these biofilms dissolves at both acidic and basic pH. This shows their biodegradability and biocompatibility behaviour. The decomposition rate of iron ion included biofilms is high compared to the normal silk fibroin biofilms. That is why these films can be used as capsules for drugs or used as soluble plasters for the treatments of herpes and mouth wounds.
- The antimicrobial experiments prove that silk fibroin has bactericidal property which is mean have bacteria killing behaviour. The effect of bacteria killing is increased as the amount of SF is increased.

- The SF particles have also bactericidal behaviour. There was a clear zone around the particles. However, the SF biofilm has no bactericidal property but has bacteriostatic behaviour that is preventing the bacteria from growing so the immune system can overcome bacteria.

5.REFERENCES

[1] Fujia Chen, David Porter, Fritz Vollrath, "Morphology and structure of silkworm cocoons", Materials Science and Engineerind C 32 (2012), 772-778.

[2] Yongzhong Wang, Hyeon-Joo Kim, Gordana Vunjak-Novakovic, David l.Kaplan, "Stem cell-based tissue engineering with silk biomaterials", Biomaterials 27 (2006), 6064-6082

[3] Qiang Zhang, Shuqin Yan, Mingzhong Li, "Silk fibroin based porous materials", Materials 2 (2009), 2276-2295.

[4] Banani Kundu, Rangam Rajkhowa, Subhas C.Kundu, Xungai Wang," Silk fibroin biomaterials for tissue regenerations", Advanced Drug Delivery Reviews (2012)

[5] Prasong Srihanam, "Application of silk based materials".Journal of Science and Technology MSU, 32 (2) , March-April 2013.

[6] Esther Wenk, Hans P.Merkle, Lorenz Meinel," Silk fibroin as a vehicle for drug delivery applications", Journal of Controlled Release, 150 (2011) 128-141.

[7] Giuliano Freddi, Raffaella Mossotti, Riccardo Innocenti," Degumming of silk fabric with several proteases ", Journal of Biotechnology 106 (2003) 101-112.

[8] Anshu B.Mathur, Vishal Gupta," Silk fibroin-derived nanoparticles for biomedical applications", Nanomedicine, 5 (5),(2010), 807-820.

[9] Zhou CZ, Confalonieri F, Medina N, Zivanovic Y, Esnault C, Yang T, Jacquet M, Janin J, Duguet M, Perasso R, Li ZG, "Fine organization of *Bombyx mori* fibroin heavy chain gene " Nucleic Acids Res, 2000;28, 2413-2419.

[10] Vollrath F, Knight DL," Liquid crystalline spinning of spider silk", Nature, 001;410,541-548.

[11] Pérez-Rigueiro J, Viney C, Llorca J, Elices M. "Silkworm silk as an engineering material", Journal of Applications of Polymeric Science, 70 (1998),2439-2447

[12] Zahn H. Silk. In: Wilks," Industrial polymers handbook: products, processes, applications", vol.4. Germany: Wiley-VCH, (2001);4:2177-2195.

[13] Keiji Numata, David L.Kaplan," Silk-based delivery systems of bioactive molecules", Advanced Drug Delivery Reviews, 62 (2010) 1497-1508.

[14] Joo-Hong Yeo, Kwang-Gill Lee, Yong-Woo Lee, Sun Yeou Kim," Simple preparetion and characteristics of silk fibroin microsphere", European Polymer Journal 39 (2003) 1195-1199.

[15] Liang CX, Hirabayashi K. Improvements of the physical properties of fibroin membranes with sodium alginate. Journal of Applications of Polymer Science, 45 (1992),1937-1943.

[16] Freddi G, Romano M. Massafra MR, Tsukada M. Silk fibroin/cellulose blend fi lms-preparation, structure and physical-properties. Journal of Applications Polymer Science, 56 (1995), 1537-1545.

[17] Aniket S.Wadajkar, Jyothi U.Menon, Tejaswi Kadapure, Richard T.Tran, Jian Yang, Kytai T.Nguyen," Design and application of magnetic-based theranostic nanoparticle system", Recent Patents on Biomedical Engineering, 6 (2013)47-57.

[18] Ren YJ, Zhou ZY, Liu BF, Xu QY, Cui FZ. Preparation and characterization of fi broin/hyaluronic acid composite scaffold. Int J Biol Macromol, 44(2009),372-378.

[19] J.Lodhia, G.Mandarano, NJ Ferris, P.Eu, SF.Cowell," Development and use of iron oxiede nanoparticles (Part 1): Synthesis of iron oxide nanoparticles for MRI", Biomedical Imaging and Intervantion Journal 2009.

[20] Sushmitha Sundar, Joydip Kundu, Subhas C Kundu," Biopolymeric nanoparticles",Science and Technology of Advanced Materials, 11 (2010).

[21] Reju Thomas, In-Kyu Park, Yong Yeon Jeong," Magnetic ıron oxide nanopaticles for multimodal imaging and therapy of cancer", Internatioal Journal of Molecular Sciences, 14 (2013), 15910-15930.

[22] www.en.wikipedia.org/ wiki/ Contrast agents

[23] www.en.wikipedia.org/wiki/Fibroin

[24] www3.nd.edu

[25] www.studyblue.com

[26] www.schoolphysics.co.uk